Analytical and Bioanalytical Chemistry (2019) 411:1569–1578
https://doi.org/10.1007/s00216-019-01598-4

RESEARCH PAPER

Application of direct analysis in real time to the study of chemical vapor generation mechanisms: identification of intermediate hydrolysis products of amine-boranes

Lucia D'Ulivo[1] · Enea Pagliano[1] · Massimo Onor[2] · Zoltan Mester[1] · Alessandro D'Ulivo[2]

Received: 6 November 2018 / Revised: 7 January 2019 / Accepted: 10 January 2019 / Published online: 28 January 2019

Abstract

In order to elucidate controversial results emerging in chemical vapor generation (CVG) for trace element determination, we conducted a series of experiments devoted to the identification of intermediates formed by acid hydrolysis of amine-boranes. For the first time, direct analysis in real time coupled with high-resolution mass spectrometry (DART-Orbitrap) was applied for detection of this class of compounds. Mass spectra of both solid amine-boranes and their aqueous solutions (pH ~ 8, no hydrolysis) were acquired for understanding their ionization pathway. Mass spectra of aqueous solutions of *t*-$BuNH_2{\cdot}BH_3$ and $Me_2NH{\cdot}BH_3$ were acquired under conditions that are employed in CVG (0.017–4.0 mol L^{-1} HCl, 0.167–0.2 mol L^{-1} borane reagent). The results disclose a reactivity driven by pH of amine-boranes undergoing hydrolysis. At low acidity, the hydrolysis proceeds according to the currently accepted displacement mechanisms (i.e., $R_3N{\cdot}BH_3 + H_3O^+ \rightarrow R_3NH^+ + H_2OBH_3$). At higher acidity, *N-tert*-butyl, cyclotriborazane, and bis(dimethylamino)boronium were identified, for the first time, during the hydrolysis of *t*-$BuNH_2{\cdot}BH_3$ and $Me_2NH{\cdot}BH_3$, respectively. Formation of these intermediates was ascribed to a hydrolysis pathway starting with the ionization of the amine-borane, (i.e., $R_3N{\cdot}BH_3 + H_3O^+ \rightarrow [(H_2O)R_3NBH_2]^+ + H_2$). The new evidence explains the anomalous behavior observed in CVG by amine-borane derivatization, and updates the currently accepted mechanisms for the acid hydrolysis of amine-boranes.

Keywords Amine-boranes · Hydrolysis · Direct analysis in real time · Mass spectrometry · Chemical vapor generation · Mechanism

Introduction

Chemical vapor generation (CVG) of gaseous hydrides and volatile metal species by aqueous boranes, MBH_4 (M = Na, K), and amine-boranes is one of the most powerful sample introduction techniques for ultra-trace determination of some elements (Ge, Sn, Pb, As, Sb, Bi, Se, Te, Hg, Zn, Hg, Cu, etc.) by atomic and mass spectrometry [1–3]. In recent years, several investigations have been devoted to CVG systems using both $NaBH_4$ (THB) and amine-boranes, $NH_3{\cdot}BH_3$ (AB), *t*-$BuNH_2{\cdot}BH_3$ (TBAB), $Me_2NH{\cdot}BH_3$ (DMAB), and $Me_3N{\cdot}BH_3$ (TMAB), in order to clarify unknown and controversial aspects related to their reactivity, in particular the mechanism of hydrolysis and hydrogen transfer [4–9].

In a recent study on CVG of H_2Se using different aqueous boranes, we found some anomalous results compared with that foreseen by the literature [10]. It was observed that the efficiency of generation of H_2Se increases in the order TBAB > AB > THB; this is an inverse correlation in comparison with CVG of SbH_3 and Hg^0 where the generation efficiency increases in the order THB > AB > TBAB [3]. Moreover, in CVG of SbH_3 and Hg^0, there is a good linear correlation between log k_i and log C_R, where k_i is the second-order rate constants of the kinetic equation $d[R_3N{\cdot}BH_3]/dt = -k_i[R_3N{\cdot}BH_3][H_3O^+]$ of the hydrolysis of amine-boranes:

Electronic supplementary material The online version of this article (https://doi.org/10.1007/s00216-019-01598-4) contains supplementary material, which is available to authorized users.

✉ Alessandro D'Ulivo
alessandro.dulivo@pi.iccom.cnr.it

[1] National Research Council Canada, 1200 Montreal Road, Ottawa, ON K1A 0R6, Canada

[2] C.N.R, Institute of Chemistry of Organometallic Compounds, S.S. of Pisa, Via. G Moruzzi, 1, 56124 Pisa, Italy

$$R_3N \cdot BH_3 + H_3O^+ \rightarrow R_3NH^+ + B(OH)_3 + 3H_2 \ (R = \text{alkyl, H}) \quad (1)$$

and C_R is the concentration of borane giving 50% generation efficiency [3].

Also, it was found [10] that the rate of hydrogen generation by the acid hydrolysis of amine-boranes (AB, TBAB, and DMAB) at acidities in the range from 0.01 to 5 mol L^{-1} H^+ was much slower than predicted using the rate constants of hydrolysis of amine-borane reported in the literature [11–13]. Furthermore, at elevated acidities (> 3 mol L^{-1} H^+), hydrogen was evolved in two distinct steps, the first being the faster one and leading to the release of about one of the three moles of hydrogen generated after complete hydrolysis [10], confirming a previous observation on AB [14].

The anomalous results obtained for CVG of H_2Se ($[H^+] >$ 0.5 mol L^{-1}) and for the acid hydrolysis of amine-boranes ($[H^+] > 0.1$ mol L^{-1}) were ascribed to the occurrence of a reaction pathway for reaction 1 that starts with the loss of molecular hydrogen [10]:

$$R_3N \cdot BH_3 + H_3O^+ \rightarrow [(H_2O)R_3NBH_2]^+ + H_2 \ (R = \text{alkyl, H}) \quad (2)$$

The ionization mechanism starting with reaction 2 differs from that involved in the currently accepted mechanism of hydrolysis of amine-boranes [11–13], which starts with the displacement of protonated amine:

$$R_3N \cdot BH_3 + H_3O^+ \rightarrow (H_2O)BH_3 + R_3NH^+ \ (R = \text{alkyl, H}) \quad (3)$$

The difference between reactions 2 and 3, which are only the first step of reaction 1, has important implications for the understanding of the mechanisms that operate in CVG. In most of the cases, the hydrolysis products of the borane reagent are the effective derivatization species generating the volatile molecule employed in the analytical determination [14].

However, the identification of borane intermediates generated during experiments lasting a few minutes, in aqueous solutions and in the presence of gas bubbles due to hydrogen evolution, is not a trivial task using spectrometric techniques such as MS, NMR, or FTIR. In this study, we applied, for the first time, the direct analysis in real time coupled with high-resolution mass spectrometry (DART-Orbitrap) to the identification of boranes species formed during the hydrolysis of amine-boranes at different acidities. Despite some limitations emerged during these studies, DART-Orbitrap experiments allow the collection of evidences that, together with those previously obtained on the rate of hydrogen evolution [10], represent a useful support to the understanding of the reactivity of amine-boranes in CVG system. Furthermore, these results reveal new aspects of the reactivity of aqueous amine-boranes not covered by the current literature.

Experimental

Borane *tert*-butylamine (TBAB) and borane dimethylamine (DMAB) complexes (assay 97%) were purchased from Sigma-Aldrich. Solutions of 0.2 mol L^{-1} TBAB and 1.0 mol L^{-1} DMAB were prepared in deionized water and were stable for several days at room temperature. Solutions of 0.1, 0.5, and 5.0 mol L^{-1} HCl were prepared from analytical grade 37% HCl.

Mass spectrometric identification of reaction intermediates was performed by using a direct analysis in real time (DART) ion source (IonSense, Saugus, MA, USA), which was positioned 17 mm away from the orifice of a LTQ linear ion trap-Orbitrap mass spectrometer working in positive ion mode (Thermo Fisher Scientific Inc., Bremen, Germany). The mass spectrometer was tuned and calibrated according to the manufacturer's operating instructions and a resolution of 30,000 was employed for all experiments. The DART was operated with helium as carrier gas at 3.5 L min^{-1} with a temperature of 80 °C and 200 °C for TBAB and DMAB, respectively. All other DART operating conditions were standard settings: needle current = 9990 mA; needle voltage = 2500 V; discharge electrode current = 7 mA; discharge electrode voltage = 149 V; grid electrode current = 10 mA; grid electrode voltage = 249 V. The lower *m*/*z* that the Orbitrap could acquire is 50.

Hydrolysis experiments were performed by mixing a volume of aqueous amine-borane with HCl solutions (see Table 1) in a 10-mL vial, under stirring.

A DIP-it™ glass stick (IonSense Inc., USA) was employed to sample the solution of amine-borane before the DART-Orbitrap analysis. The glass stick was dipped into the solution at regular intervals over the range of reaction times from 10 to 600 s and exposed to the DART ion source in order to collect a scan of the investigated amine-borane solution. Signal acquisition was performed with Xcalibur Thermo Tune Plus software (Thermo Fisher Scientific). For the collection of the mass spectra of the solid, the glass stick was dipped several times into the solid reagents until a few crystals were collected on its surface. At this point, such crystals were exposed to the DART. For both the solutions and the solid reagents, the signal acquisition was started about 30 s before sample exposure and terminated about 30 s after removal of the sample from the ion source.

Results

DART mass analysis of amine-boranes in solid form and in aqueous solution

Positive ion, DART-Orbitrap mass spectra were obtained for both solid and aqueous solution (pH ~ 8) of amine-boranes. The results are reported in Table 2 for TBAB and in Table 3 for DMAB.

Table 1 Reaction conditions for hydrolysis of amine-boranes

Amine-borane	HCl			Reaction conditions		
	V (mL)	Conc. (mol L^{-1})	Amount (mmol)	HCl conc. (mol L^{-1})	$R_2NH{\cdot}BH_3$ (mol L^{-1})	HCl/borane (mol/mol)
1 mL of 0.2 mol L^{-1} tBuNH$_2$BH$_3$ (0.2 mmol TBAB)	0.2	0.1	0.02	1.67×10^{-2}	1.67×10^{-1}	0.1
	0.2	0.5	0.1	8.3×10^{-2}	1.67×10^{-1}	0.5
	0.1	5.0	0.5	0.45	1.82×10^{-1}	2.5
0.5 mL of 1.0 mol L^{-1} Me_2NHBH_3 (0.5 mmol DMAB)	2	0.1	0.2	8.0×10^{-2}	0.2	0.4
	2	0.5	1.0	0.4	0.2	2.0
	2	5.0	10	4.0	0.2	20

The spectra do not exhibit intense signals for the expected $[M + H]^+$ ion or the molecular ion $M^{+\bullet}$. As already reported for alkanes [15] and methylarsanes [16], the most characteristic signals associated with the amine-borane molecules, $R_3N{\cdot}BH_3$ (R = alkyl, H), are those arising from the hydride abstraction. Both TBAB and DMAB ionized positively giving the characteristics signals at m/z $[M - H^-]^+$, $C_4H_{13}NB^+$ (**3a**, Table 2) and $C_2H_9NB^+$ (**2b**, Table 3), respectively. The amine-borane cations can evolve by further hydride loss and the replacement of the hydride by hydroxyl group (**4a** and **5a** for TBAB, Table 2; **3b** and **4b** for DMAB, Table 3). The protonated amine is well detectable for TBAB (**2a**, Table 2) but not for DMAB because the molecular weight of $Me_2NH_2^+$ is < 50 Da. This evidence indicates that in DART the most likely ionization pathways for amine-boranes can be schematized as follows (Scheme 1):

Other pathways seem to be related to the identity of amine. The borane cation of DMAB evolves by dihydrogen loss giving **1b** (Table 3), a pattern that was not observed for TBAB. For TBAB, the formation of dimeric species (**7a**, **8a**, **9a**, Table 2) that are not observed for DMAB was instead evident.

Time evolution of mass spectra during hydrolysis of amine-boranes

The similarities between the ionization pathways taking place in DART (Scheme 1) and those taking place during hydrolysis (reactions 2 and 3) indicate that amine-boranes in DART undergo a process that could be defined as a hydrolysis in gaseous phase. For this reason, a particular attention was dedicated to the evaluation of mass spectra under hydrolysis conditions in order to identify possible artifacts or interferences.

The DART-Orbitrap mass spectra obtained during hydrolysis are reported in Table 4 for TBAB and in Table 5 for DMAB.

Depending on the acidity, the mass spectra of amine-borane during hydrolysis present some striking differences compared with those obtained in aqueous solution and, as an important feature, they present a temporal evolution.

Figure 1 compares the mass spectrum of TBAB in aqueous solution (Fig. 1a) with that obtained after 30 s hydrolysis in 0.45 mol L^{-1} HCl (Fig. 1b). The boron-

Table 2 DART-Orbitrap full scan mass spectra of TBAB, in solid and in aqueous solution (pH ~ 8)

	Detected ions[(a)]	Abundance (%)		Detected mass (Da)	Exact mass (Da)	$\Delta m/m$ (ppm)	Proposed structure
		Solid	Solution				
1a	$C_4H_9^+$	16	20	57.0688	57.0704	− 28	$(CH_3)_3C^+$
2a	$C_4H_{12}N^+$	100	100	74.0954	74.0970	− 22	$(CH_3)_3C\text{-}NH_3^+$
3a	$C_4H_{13}N^{11}B^+$	0.7	2.1	86.1125	86.1141	− 10	$(CH_3)_3C\text{-}NH_2\text{-}BH_2^+$
4a	$C_4H_{13}NO^{11}B^+$	4.0	7.2	102.1074	102.1090	− 16	$(CH_3)_3C\text{-}NH_2\text{-}BHOH^+$
5a	$C_4H_{13}NO_2{}^{11}B^+$	1.4	3.9	118.1024	118.1039	− 13	$(CH_3)_3C\text{-}NH_2\text{-}B(OH)_2^+$
6a	$C_8H_{24}N_2{}^{11}B$	60	nd	159.2020	159.2032	− 8	[**2a** + $Me_3C\text{-}NH_2\text{-}BH_3$]$^+$ or [**3a** + $(CH_3)_3C\text{-}NH_2$]$^+$
7a	$C_8H_{27}N_2{}^{11}B^{11}B^+$	0.8	1	173.2346	173.2360	− 8	Dimeric species $Me_3C\text{-}NH_2\text{-}BH_3$ + **3a**
8a	$C_8H_{27}N_2O^{11}B^{11}B^+$	20	22	189.2295	189.2309	− 7	Dimeric species $Me_3C\text{-}NH_2\text{-}BH_3$ + **4a**
9a	$C_8H_{27}N_2O_2{}^{11}B^{11}B^+$	2	5	205.2245	205.2259	− 7	Dimeric species $Me_3C\text{-}NH_2\text{-}BH_2OH$ + **4a**

[(a)] For all B-containing ion, the isotope pattern on boron was confirmed

Table 3 DART-Orbitrap full scan mass spectra of DMAB, in solid and in aqueous solution (pH ~ 8)

Detected ions[c]		Abundance (%)		Detected mass (Da)	Exact mass (Da)	$\Delta m/m$ (ppm)	Assigned structure
		Solid	Solution				
1b	$C_2H_7N^{11}B^+$	16	12	56.0658	56.0671	− 23	$Me_2N{=}BH^+$
2b	$C_2H_9N^{11}B^+$	13	10	58.0814	58.0826	− 21	$Me_2NH\text{-}BH_2^+$
3b	$C_2H_9NO^{11}B^+$	100	100	74.0764	74.0777	− 18	$Me_2NH\text{-}BHOH^+$
4b	$C_2H_9NO_2{}^{11}B^+$	21	5.0	90.0713	90.0726	− 15	$Me_2NH\text{-}B(OH)_2^+$
5b	$C_2H_{10}NO_2{}^{11}B^{11}B^+$	n.d.	0.6 (6)[a]	102.0885	102.0898	− 13	**[6c** − H^-**]**$^+$ and/or **[6d** − H^-**]**$^{+(b)}$

[a] Measured during hydrolysis in 0.4 mol L^{-1} HCl, 30-s reaction time. [b] See Scheme 2. See Electronic Supplementary Material (ESM), Fig. S1 for mass spectrum of **5b**. [c] For all B-containing ion, the isotope pattern on boron was confirmed

containing ions **10a**, **11a**, and **12a** (see ESM, Fig. S3, for mass spectra of **12a**) and the ion **10x**, which does not contain boron, are the most abundant species; these species were not detected in aqueous solution nor in the solid reagent. At the same time, the ions from **3a** to **9a** detected from aqueous solution and arising from ionization of TBAB (Fig. 1a and Table 2) were not present under these hydrolysis conditions. Molecular formulae could be assigned (Table 4) to the ions at *m/z* 184.2142 (**10a**), 201.1840 (**10x**), 240.2768 (**11a**), and 254.3056 (**12a**).

Table 4 summarizes ions detected during hydrolysis of TBAB in 0.45 mol L^{-1} HCl. No ions other than those reported in Table 4 were observed during hydrolysis using other acidity conditions (1.67×10^{-2} and 8.3×10^{-2} mol L^{-1} HCl). Ion **12a** is the product of hydride abstraction from the *N-tert*-butyl, cyclotriborazane, **12**. Ions **11a** and **10a** are most likely formed in the DART source by sequential loss of borane and *tert*-butyl fragments from **12**, respectively (Table 4).

While these species are not detectable at low acidities (Fig. 2a), their appearance and disappearance in the mass spectra are well correlated with the reaction time at higher acidities (Fig. 2b). This evidence strongly supports the hypothesis that **12** is a species that exists in solution and is formed during hydrolysis of TBAB, whereas **10a** and **11a** are species that are formed from **12** in the DART source.

Figure 3 compares mass spectra of DMAB in aqueous solution and during hydrolysis in 0.4 mol L^{-1} HCl at 10- and 60-s reaction times. At 60 s, the mass spectra are dominated by ion **6b** (Fig. 3c) that is also detectable at 10 s (relative abundance about 0.8% (Fig. 3b), but not in aqueous solution (Fig. 3a and Table 2) or in the solid reagent (Table 2). Ion **5b** is also present in the mass spectrum of an aqueous solution, even if at lower relative abundance, but not in that of the solid (Table 2). By increasing the acidity to 4.0 mol L^{-1} HCl, new ions appear at *m/z* 74.0589 Da (**7x**), 91.1221 Da (**8b**), 128.1023 Da (**9b**), and 163.0750 Da (**10b**), but none of these contains boron (Table 5). The relative abundance of the ions observed in the mass spectrum of DMAB changes with the reaction time and hydrolysis conditions, as shown in Fig. 4.

The most interesting boron-containing species is ion **6b**. It is detectable only after 6-min hydrolysis in 0.08 mol L^{-1} HCl (relative abundance about 3%, Fig. 4a), while it becomes the most abundant ion from 60- to 300-s reaction time in 0.4 mol L^{-1} HCl (Fig. 4b). No ions other than those reported in Table 5 were observed during hydrolysis using lower acidity conditions (8.0×10^{-2} mol L^{-1} HCl).

Under strong acidic conditions (4.0 mol L^{-1} HCl, Fig. 4c), **6b** is detected after 30-s hydrolysis as the major species that disappears rather quickly from the mass spectrum. Ion **6b** is therefore related to a species formed during hydrolysis of DMAB, that is, bis-dimethylamine boronium itself, $(Me_2NH)_2BH_2^+$.

Ion **5b** can be detected in aqueous solution (about 0.6%, Table 2), but its relative abundance remained low even during hydrolysis in both 0.08 and 0.4 mol L^{-1} HCl (< 6%; Fig. 4a, b). However, species **5b** is undetectable during hydrolysis in 4.0 mol L^{-1} HCl. Possibly, **5b** can be generated in the DART source by hydride abstraction from both species **6c** and **6d** (Table 3), which, in turn, could be formed during hydrolysis of DMAB.

In conclusion, the time evolution of mass spectra during hydrolysis, using various acidic conditions, permits the selection of at least two species formed during hydrolysis, **12** from TBAB and **6b** from DMAB, and not from artifacts in the DART source. The appearance of species **12** and **6b** during hydrolysis is almost simultaneous with the disappearance of the amine-borane, confirming that **12** and **6b** are species arising from reactions involving the original substrate.

Scheme 1 DART ionization pathways for DMAB and TBAB

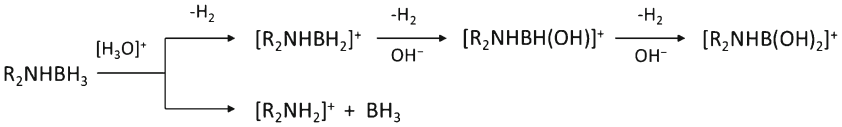

Scheme 2 Proposed structure of selected species detected by DART-Orbitrap (see ESM for mass spectra, Figs. S1–S3)

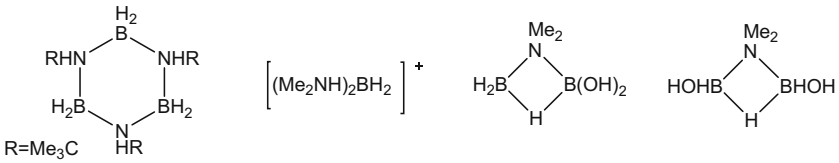

12 **6b** **6c** **6d**

Limitations of DART-Orbitrap experiments

Not all the species that are formed during hydrolysis experiments could be detected by DART-Orbitrap due to ionization and/or volatilization limitations or being outside of the mass range of the Orbitrap (< 50 Da). In the hydrolysis at low acidities, for TBAB, the displacement of amine forms **2a** (tBuNH$_3^+$) whereas in the hydrolysis of DMAB, the protonated amine $Me_2NH_2^+$ could not be detected (< 50 Da). For both TBAB and DMAB, the species $BH_3(H_2O)$ and its hydrolysis products $(H_2O)BH_2OH$ and (H_2O) BH $(OH)_2$ were outside the Orbitrap mass range. In this case, the hydrolysis pathway starting with reaction 3 could not be fully supported by direct evidence. Considering the data on the rate of hydrogen evolution [10], it can be concluded that, at low acidities, there is no evidence against the proposed hydrolysis pathway starting with reaction 3.

A further evidence indicating that not all the species present in solution are detected is the hydrolysis of DMAB in 4.0 mol L^{-1} HCl. In this case, no boron-containing ions were detectable after 90-s hydrolysis. According to the experimental data, under these conditions, the hydrolysis of DMAB is far from completion, as about 60–70% of the total available hydrogen is evolved at 90–120-s reaction time [10]. This means that a significant fraction of hydrolysable borane species are still present in solution, but they were not detected by DART-Orbitrap.

Discussion

The hydrolysis behavior of amine-boranes

Details of the displacement mechanism starting with reaction 3 are reported in Scheme 3.

The displacement of protonated ammine is the rate determining step of hydrolysis. The above mechanism of amine-boranes was proposed and supported by evidence reported by Ryschkewitsch [12] and by Kelly et al. [11, 13].

The ionization mechanism of hydrolysis of amine-boranes starting with reaction 2 is similar to the one described by Kreevoy and Hutchins for the hydrolysis of $NaBH_4$ and $NaBH_3CN$ (Scheme 4) and proposed by the authors also for the hydrolysis of amine-boranes [8, 17, 18]:

Even if the displacement mechanism for the hydrolysis of amine-boranes according to Scheme 3 appears to be accepted in the literature [8, 19, 20], there are several reasons indicating that the mechanism of hydrolysis of amine-boranes presented some controversial aspects. Kelly and Marriot, who proposed the displacement mechanism, in their study on the reexamination of the mechanism of hydrolysis of AB [13], did not exclude the occurrence of a hydrolysis pathway according to Scheme 4, but they conclude that the achieved experimental evidences were difficult to reconcile with such a reaction scheme. The kinetics experiments conducted by Kelly and Marriot were performed in the range from pH/pD from 4.3 to 6.1 [13], very far from the CVG conditions that gave the anomalous results described above [10]. Furthermore, on the

Table 4 DART-Orbitrap full scan mass spectra of TBAB in 0.45 M HCl (reaction time 30 s. Species **3a**, **4a**, **5a**, **6a**, **7a**, **8a**, and **9a** reported in Table 2 were not detected. No ions other than those reported in this table were observed during hydrolysis using other acidity conditions (1.67×10^{-2} and 8.3×10^{-2} mol L^{-1} HCl))

Detected ions[c]		Abundance (%)	Detected mass (Da)	Exact mass (Da)	$\Delta m/m$ (ppm)	Assigned structure
1a	$C_4H_9^+$	22	57.0688	57.0704	−28	$(CH_3)_3C^+$
2a	$C_4H_{12}N^+$	27	74.0954	74.0970	−25	$(CH_3)_3C\text{-}NH_3^+$
10a	$C_8H_{24}N_3{}^{11}B^{11}B^+$	67	184.2142	184.2156	−8	[**11a** − Me_3C^+ + H^+]$^+$
10x	$C_{12}H_{25}O_2^+$	94	201.1840	201.1849	−4.5	Tentative molecular formula
11a	$C_{12}H_{32}N_3{}^{11}B^{11}B^+$	100	240.2768	240.2782	−4	[**12a** − BH_3]$^+$
12a	$C_{12}H_{35}N_3{}^{11}B^{11}B^{11}B^+$	50	254.3096	254.3110	−6	[**12** − H^-]$^{+(b)}$ Not detected in solid or aqueous solution (Table 2)

[b] See Scheme 2. [c] For all B-containing ion, the isotope pattern on boron was confirmed

Table 5 DART-Orbitrap full scan mass spectra of DMAB under acidic conditions

Detected ions		Abundance (%)	Detected mass (Da)	Exact mass (Da)	$\Delta m/m$ (ppm)	Assigned structure
HCl = 0.4 mol L^{-1}, reaction time 300 s						
1b	$C_2H_7N^{11}B^+$	2.1	56.0658	56.0672	− 25	$Me_2N{=}BH^+$
2b	$C_2H_9N^{11}B^+$	3.2	58.0814	58.0828	− 24	$Me_2NH\text{-}BH_2^+$
3b	$C_2H_9NO^{11}B^+$	5.9	74.0764	74.0777	− 18	$Me_2NH\text{-}BHOH^+$
4b	$C_2H_9N^{11}BO_2^+$	(12)[a]	90.0713	90.0726	− 14	$Me_2NH\text{-}B(OH)_2^+$
5b	$C_2H_{10}NO_2{}^{11}B^{11}B^+$	0.2	102.0885	102.0898	− 13	See Table 3
6b	$C_4H_{16}N_2{}^{11}B^+$	100	103.1396	103.1407	− 11	$(Me_2NH)_2BH_2^+$ Not detected in solid or aqueous solution (Table 3)
HCl = 4.0 mol L^{-1}, reaction time 120 s and 300 s						
7x	$C_3H_8NO^+$	(40)[b]	74.0589	74.0606	− 23	Tentative molecular formula
8b	$C_4H_{15}N_2^+$	21	91.1221	91.1235	− 15	HCl loss from **9b** Detected only in 4.0 mol L^{-1} HCl
9b	$C_4H_{16}N_2{}^{35}Cl$	100	127.0992	127.1002	− 8	Detected only during hydrolysis in 4.0 mol L^{-1} HCl
10b	$C_8H_9N_3O^+$	(100)[b]	163.0750	163.7546	+ 2	Detected only in 4.0 mol L^{-1} HCl

[a] Reaction time 30 s. [b] Reaction time 300 s

contrary of ionization mechanism of Scheme 4, the displacement mechanism of Scheme 3 is not able to explain the H-D exchange which prevails on hydrolysis at elevated acidities in more hydrolytic stable amine-boranes [21].

The evidence obtained in this work, integrated with those on the rate of hydrogen evolution reported recently [10], indicates that the displacement mechanism (Scheme 3) is not able to explain the behavior of amine-boranes at increasing acidities. In particular, it appears evident that, depending on acidity, the hydrolysis of amine-boranes can take place following two different reaction pathways. At low acidities, the displacement of protonated amine takes place according to Scheme 3, whereas by increasing the acidity the hydrolysis starts with the ionization of amine-borane, similarly according to reaction 4. However, even the mechanisms of hydrolysis reported in Scheme 4 cannot explain the formation of **12** and **6b** species.

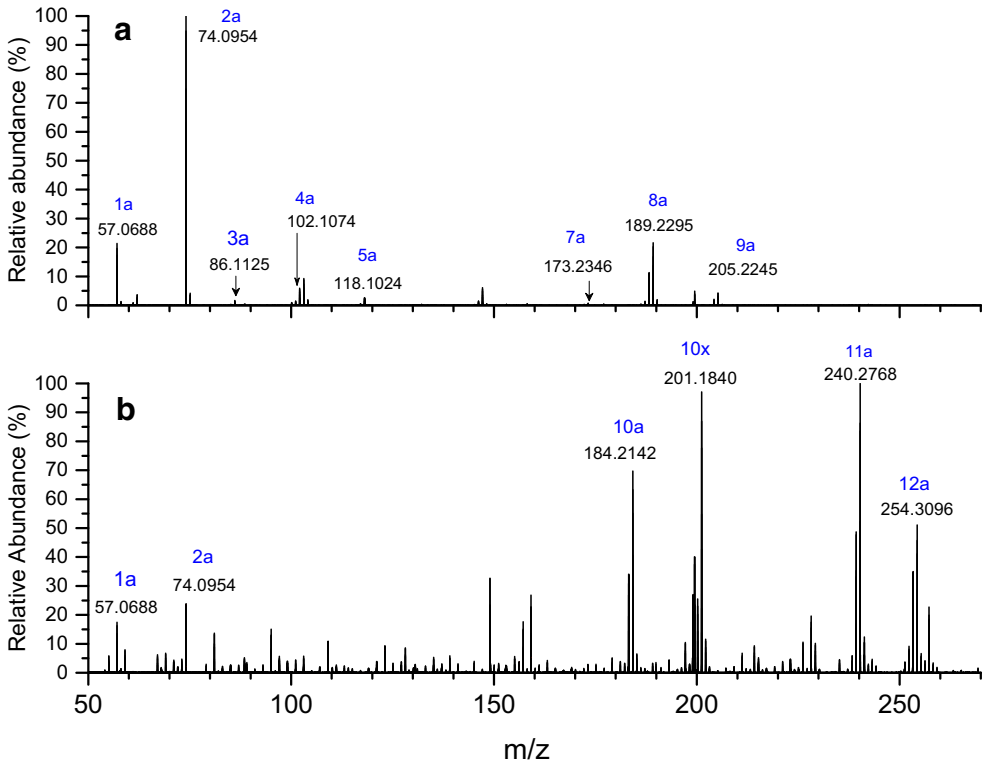

Fig. 1 Comparison of mass spectra of 1.67 × 10–1 mol L^{-1} TBAB in aqueous solution (**a**) and during hydrolysis in 0.45 mol L^{-1} HCl at reaction time of 30 s (**b**). See Tables 2 and 4 for molecular formula and Scheme 2 for structures. See ESM, Fig. S3, for mass spectra of **12a**. Instrumental conditions for DART-MS are reported in the "Experimental" section

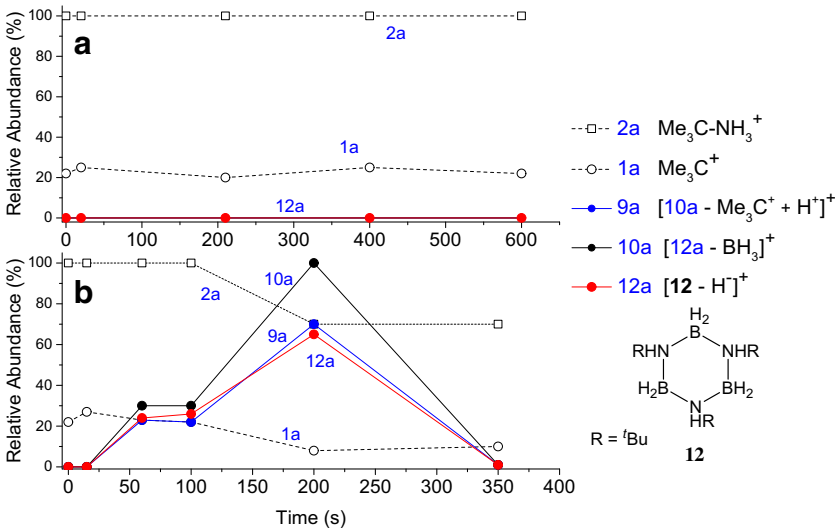

Fig. 2 DART-MS measurements. Variation of the relative abundance of selected ions during the hydrolysis of TBAB in 1.67×10^{-2} (**a**) and 8.3×10^{-2} mol L^{-1} HCl (**b**). **12** is detected as three different ions, **12a**, **10a**, and **9a**, arising from the indicated fragment losses (see ESM). Instrumental conditions for DART-MS are reported in the "Experimental" section

The only reasonable hypothesis is that, at high acidity, the hydrolytic stable boronium species [22] reacts preferentially with the amine-borane forming dimeric species which can evolve both by rearrangement of further polymerization reactions. This hypothesis fits with the evidence that amine-borane was disappearing from solution during the formation of either **12** or **6b** (Figs. 1, 2, 3, and 4). This type of reactivity is closer to that of amine-boranes undergoing dehydrogenation using various types of catalysts in organic media. The formation of **12** and similar cyclotriborazanes is reported in dehydrocoupling reactions of TBAB and other primary amine-boranes with various types of catalysts [19, 20, 23, 24] whereas the formation of boronium cation **6b** is reported in the dehydrocoupling of DMAB using Pt^{II} complexes [25]. Stephens et al. [26] investigated dehydrogenation of ammonia borane initiated by either Brønsted or Lewis acids in organic solvents and described details of the mechanism of the reaction:

$$3H_3N \cdot BH_3 + \text{acid} \rightarrow [\text{intermediates}] \rightarrow H_2 + \left[BH_2(NH_3)_2\right]^+ + B_2H_5(\mu\text{–}NH_2) \quad (4)$$

where the boronium species, $[BH_2(NH_3)_2]^+$, is similar to **6b**.

One important conclusion of Stephens et al. [26] on the mechanism of acid-initiated dehydrogenation of ammonia borane was that the reaction starts most likely with the formation of a boronium species, according to a reaction similar to 2. We believe that the occurrence of similar mechanisms, originating with the formation of boroniun

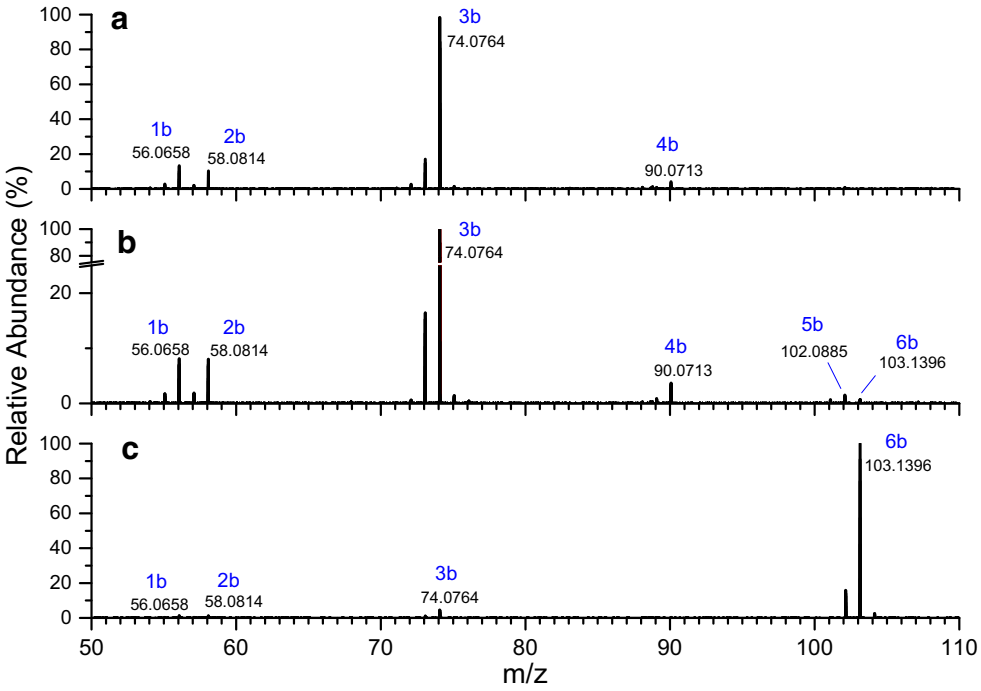

Fig. 3 Mass spectra of 0.2 mol L^{-1} DMAB in aqueous solution (**a**) and during hydrolysis in 0.4 mol L^{-1} HCl at reaction time of 10 s (**b**) and 60 s (**c**). See Tables 3 and 5 for molecular formulae and structure. See ESM, Fig. S2, for mass spectra of **6b**. Instrumental conditions for DART-MS are reported in the "Experimental" section

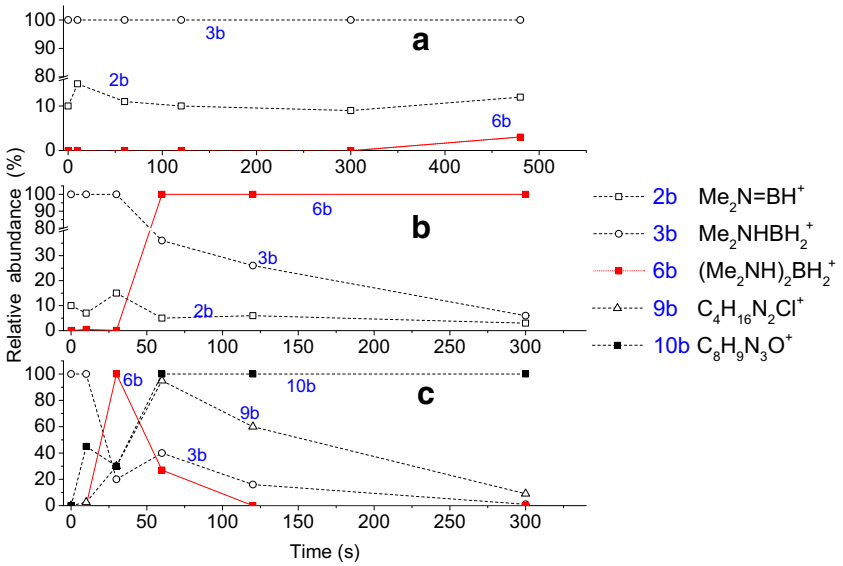

Fig. 4 Variation of the relative abundance of selected ions (see Tables 3 and 5) during the hydrolysis of 0.2 mol L^{-1} DMAB in 0.08 mol L^{-1} HCl (**a**), 0.4 mol L^{-1} HCl (**b**), and 4.0 mol L^{-1} HCl (**c**). Instrumental conditions for DART-MS are reported in the "Experimental" section

species at elevated acidities, causes the deviations from the kinetics and mechanisms of hydrolysis of aqueous amine-boranes which are proposed in the literature (Schemes 3 and 4). The acid hydrolysis behavior of amine-boranes, which is consistent with the available experimental evidences, can be summarized in the following reaction scheme (Scheme 5):

Mechanism of CVG using amine-boranes

The interpretation of the reactivity of the analytical substrates of Hg^{II} [3], Sb^{III} [3, 6, 9], Bi^{III} [6], Sn^{IV} [9], As^{III}, As^{V}, methylarsenic^{V} acids [6, 7], and Se^{IV} [10, 27] undergoing CVG to hydrides by amine-boranes must be revised in light of the herein reported evidence. In particular, it is of interest for the elucidation of CVG mechanisms to understand which borane species can play a role in the derivatization reaction.

Depending on acidity, different borane intermediates are formed during CVG by aqueous boranes.

At low acidity, i.e., pH > 2, the amine-boranes, $R_3N{\cdot}BH_3$ (R = alkyl, H), hydrolyzes slowly according to reaction pathway **I** (Scheme 5), which is the displacement mechanism of Scheme 3. In this case, the derivatizing species can be $R_3N{\cdot}BH_3$, the amine-borane itself, $BH_3(H_2O)$, and the hydridoboron species arising from its hydrolysis, $(H_2O)BH_2OH$ and $(H_2O)BH(OH)_2$ [8, 28]. The hydrolysis products of amine-boranes at low acidities are therefore the same that are formed from hydrolysis of BH_4^-. However, in this case, their rate of formation is controlled by the displacement of protonated amine, which in this case coincides with k_i, the second-order rate constant of the kinetic equation [8, 28] (see the "Introduction" section).

By increasing the acidity, the amine-borane starts to be ionized according to reaction pathway **II** (Scheme 5) forming borane cations, $[R_3NBH_2]^+$ (R = alkyl, H), and other B-H containing species that are formed by a series of polymerization and/or rearrangements starting with the reaction of $[R_3NBH_2]^+$ with $R_2NH{\cdot}BH_3$. In strong acidic conditions ($[H^+] > 1$ mol L^{-1}), ionization of amine-boranes like TBAB and AB is as fast as the mixing step or reagent [10] and, most likely, the slowly hydrolyzing $[R_3NBH_2]^+$ and its derivatives, such as **12** and **6b**, are the most abundant species available for CVG derivatization.

Scheme 3 Hydrolysis mechanism proposed by Kelly et al. [11, 13] and Ryschkewitsch [12]

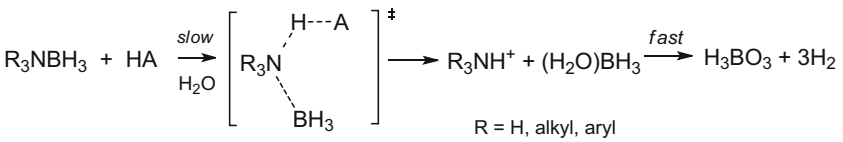

Scheme 4 Hydrolysis mechanism proposed by Kreevoy and Hucthins [17, 18]

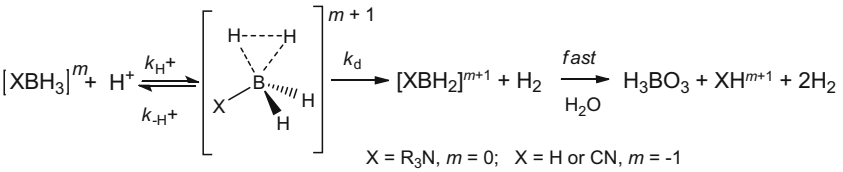

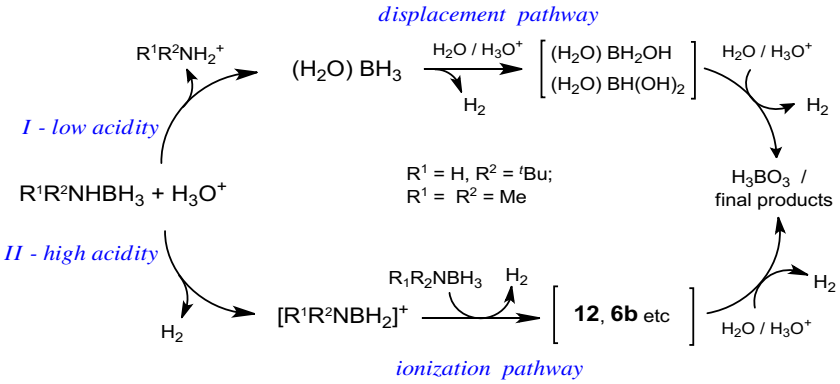

Scheme 5 Acid hydrolysis reaction pathways of amine-boranes

Conclusions

The use of DART-Orbitrap allowed the detection of amine-boranes both in solid and in near aqueous solutions, highlighting the unique capability of this analytical arrangement to interrogate multiphase, non-dilute systems often in harsh pH conditions. Amine-boranes, in solid or in aqueous solution (pH ~ 8), exhibited an ionization pathway that starts with both the displacement of protonate amine and with the hydride abstraction, the latter behavior being similar to alkanes [15] and arsanes [16]. Striking differences are observed for mass spectra of amine-boranes during hydrolysis under various acidic conditions. We identified *N-tert*-butyl, cyclotriborazane, and bis(dimethylamino)boronium cation during the hydrolysis of TBAB and DMAB, respectively. The formation of these intermediates could not be justified by the currently proposed mechanism of hydrolysis reported in the literature [11–13, 17]. The evidences obtained in the present work along with those reported recently [10] highlight the current limits on the knowledge of the mechanisms that govern the acid hydrolysis of the amine-boranes. In particular, a single mechanism could not explain the hydrolysis of amine-boranes in a wide range of acidity, $0 < pH < 6$. The mechanisms starting with the displacement of the amine ($R_3N{\cdot}BH_3 + H_3O^+ \rightarrow R_3NH^+ + BH_3(H_2O)$) [11–13] and the ionization reaction ($R_3N{\cdot}BH_3 + H_3O^+ \rightarrow [(H_2O)R_3NBH_2]^+ + H_2$) [17] can coexist and they can explain the apparent anomalous results reported recently both in CVG of H_2Se and in kinetics of amine-boranes hydrolysis [10]. At low acidity, the displacement mechanism **I** (Scheme 5) prevails, whereas by increasing the acidity, the hydrolysis of amine-borane is governed by the ionization mechanism **II** (Scheme 5). The intermediate boranes/hydridoboron species formed in the different hydrolysis pathways play a decisive role in determining the reactivity of a CVG system.

Our results represent a further confirmation that the borane reagents ($NaBH_4$, $R_3N{\cdot}BH_3$) employed in CVG of volatile species are not the only reactive molecules in the hydride generation, but another plethora of boranes intermediates may enter the CVG reactivity and be better suited for the formation of volatile species of certain elements [8].

Compliance with ethical standards

Conflict of interest The authors declare that they have no competing interests

Publisher's note Springer Nature remains neutral with regard to jurisdictional claims in published maps and institutional affiliations.

References

1. Dědina J, Tsalev DL. Hydride generation atomic absorption spectrometry. Chichester: Wiley; 1995.
2. Sturgeon RE, Mester Z. Analytical applications of volatile metal derivatives. Appl Spectrosc. 2002;56:202A–13A.
3. D'Ulivo A, Loreti V, Onor M, Pitzalis E, Zamboni R. Chemical vapor generation atomic spectrometry using amineboranes and cyanotrihydroborate (III) reagents. Anal Chem. 2003;75:2591–600.
4. Bramanti E, Lomonte C, Onor M, Zamboni R, D'Ulivo A, Raspi G. Mercury speciation by liquid chromatography coupled with on-line chemical vapour generation and atomic fluorescence spectrometric detection (LC-CVGAFS). Talanta. 2005;66:762–8.
5. D'Ulivo A, Mester Z, Meija J, Sturgeon RE. Mechanism of generation of volatile hydrides of trace elements by aqueous tetrahydroborate (III). Mass spectrometric studies on reaction products and intermediates. Anal Chem. 2007;79:3008–15.
6. Welna M, Zyrnicki W. Investigation of simultaneous generation of arsenic, bismuth and antimony hydrides using inductively coupled plasma optical emission spectrometry. Anal Lett. 2011;44:942–53.
7. Pitzalis E, Onor M, Mascherpa MC, Pacchi G, Mester Z, D'Ulivo A. Chemical generation of arsane and methylarsanes with amine boranes. Potentialities for nonchromatographic speciation of arsenic. Anal Chem. 2014;86:1599–607.
8. D'Ulivo A, Dědina J, Mester Z, Sturgeon RE, Wang Q, Welz B. Mechanisms of chemical generation of volatile hydrides for trace element determination (IUPAC Technical Report). Pure Appl Chem. 2011;83:1283–340.
9. D'Ulivo A, Baiocchi C, Pitzalis E, Onor M, Zamboni R. Chemical vapor generation for atomic spectrometry. A contribution to the comprehension of reaction mechanisms in the generation of volatile hydrides using borane complexes. Spectrochim Acta B. 2004;59:471–86.
10. D'Ulivo L, Spiniello R, Onor M, Campanella B, Mester Z, D'Ulivo A. Behavior and kinetic of hydrolysis of amine boranes in acid media employed in chemical vapor generation. Anal Chim Acta. 2018;998:28–36.
11. Kelly HC, Marchelli FR, Giusto MB. The kinetics and mechanism of solvolysis of amineboranes. Inorg Chem. 1964;3:431–7.

12. Ryschkewitsch GE. Amine boranes. I. Kinetics of acid hydrolysis of trimethylamine borane. J Am Chem Soc. 1960;82:3290–4.
13. Kelly HC, Marriott VB. Reexamination of the mechanism of acid-catalyzed amine-borane hydrolysis. The hydrolysis of NH_3•BH_3. Inorg Chem. 1979;18:2875–8.
14. D'Ulivo A, Onor M, Pitzalis E. Role of hydroboron intermediates in the mechanism of chemical vapor generation in strongly acidic media. Anal Chem. 2004;76:6342–52.
15. Cody RB. Observation of molecular ions and analysis of nonpolar compounds with the direct analysis in real time ion source. Anal Chem. 2009;81:1101–7.
16. Pagliano E, Onor M, McCooeye M, D'Ulivo A, Sturgeon RE, Mester Z. Application of direct analysis in real time to a multiphase chemical system: identification of polymeric arsanes generated by reduction of monomethylarsenate with sodium tetrahydroborate. Int J Mass Spectrom. 2014;371:42–6.
17. Kreevoy MM, Hutchins JEC. H_2BH_3as an intermediate in tetrahydridoborate hydrolysis. J Am Chem Soc. 1972;94:6371–6.
18. Kreevoy MM, Hutchins JEC. Acid-catalyzed hydrolysis and isotope exchange in LiBH3CN. J Am Chem Soc. 1969;91:4329–30.
19. Stephens FH, Pons V, Tom Baker R. Ammonia–borane: the hydrogen source par excellence? J Chem Soc Dalton Trans. 2007;39:2613–26.
20. Johnson HC, Hooper TN, Weller AS. The catalytic dehydrocoupling of amine–boranes and phosphine–boranes. Top Organomet Chem. 2015;49:153–220.
21. Davis RE, Brown AE, Hopmann R, Kibby CL. A rapid and quantitative exchange of the boron hydrogens in thrimethylamine borane with D2O. J Am Chem Soc. 1963;85:497.
22. Miller NE, Muetterties EL. Chemistry of boranes. X. Borane cations, $H_2B(base)^{2+}$. J Am Chem Soc. 1964;86:1033–8.
23. Melen RL. Dehydrocoupling routes to element–element bonds catalysed by main group compounds. Chem Soc Rev. 2016;45:775–88.
24. Jaska CA, Temple K, Lough AJ, Manners I. Transition metal-catalyzed formation of boron-nitrogen bonds: catalytic dehydrocoupling of amine-borane adducts to form aminoboranes and borazines. J Am Chem Soc. 2003;125:9424–34.
25. Roselló-Merino M, López-Serrano J, Conejero S. Dehydrocoupling reactions of dimethylamine-borane by Pt (II) complexes: a new mechanism involving deprotonation of boronium cations. J Am Chem Soc. 2013;135:10910–3.
26. Stephens FH, Baker RT, Matus MH, Grant DJ, Dixon DA. Acid initiation of ammonia-borane dehydrogenation for hydrogen storage. Angew Chem Int Ed. 2007;46:746–9.
27. Pitzalis E, Onor M, Spiniello R, Braz CEM, D'Ulivo A. Mechanism of action of additives in chemical vapor generation of hydrogen selenide: iodide and thiocyanate. Spectrochim Acta B. 2018;145:122–31.
28. D'Ulivo A. Chemical vapor generation by tetrahydroborate (III) and other borane complexes in aqueous media: a critical discussion of fundamental processes and mechanisms involved in reagent decomposition and hydride formation. Spectrochim Acta B. 2004;59:793–825.